Nanostructural evidence at the phase boundary of A- and C-type antiferromagnetic phases in $Nd_{1-x}Sr_xMnO_3$ crystals

2007 J. Phys.: Condens. Matter 19 492201

(http://iopscience.iop.org/0953-8984/19/49/492201)

IOP FTC

IOP PUBLISHING JOURNAL OF PHYSICS: CONDENSED MATTER

J. Phys.: Condens. Matter **19** (2007) 492201 (7pp) doi:10.1088/0953-8984/19/49/492201

FAST TRACK COMMUNICATION

Nanostructural evidence at the phase boundary of A- and C-type antiferromagnetic phases in $Nd_{1-x}Sr_xMnO_3$ crystals

M Nagao[1,2], T Asaka[1], D Akahoshi[3], R Hatakeyama[3], T Nagai[1], M Saito[1], K Watanabe[1], M Tanaka[1], A Yamazaki[2], T Hara[1], K Kimoto[1], H Kuwahara[3] and Y Matsui[1]

[1] National Institute for Materials Science, Tsukuba 305-0044, Japan
[2] Graduate School of Science and Engineering, Waseda University, Tokyo 169-8555, Japan
[3] Department of Physics, Sophia University, Tokyo 102-8554, Japan

E-mail: NAGAO.Masahiro@nims.go.jp

Received 4 September 2007
Published 15 November 2007
Online at stacks.iop.org/JPhysCM/19/492201

Abstract

A weak ferromagnetic phase appears around the phase boundary between the A-type and C-type antiferromagnetic phases in overdoped $Nd_{1-x}Sr_xMnO_3$ crystals ($0.6 \leqslant x \leqslant 0.7$). We investigated the crystal structure and the magnetic domain structure around the phase boundary, by powder synchrotron x-ray diffractometry and transmission electron microscopy. The phase boundary exists between $x = 0.62$ in the phase separation region where the A-type and C-type antiferromagnetic phases coexist and $x = 0.625$ in the C-type antiferromagnetic phase. By transmission electron microscopy, the orbital-disordered nanodomains in the C-type antiferromagnetic matrix phase were only observed in the vicinity of the phase boundary in the C-type antiferromagnetic phase. This is a nanoscale inhomogeneity but is not a conventional phase separation for manganites. We also successfully observed magnetic domain structures in the weak ferromagnetic phase by Lorentz electron microscopy. Moreover, we found that the ferromagnetic correlation becomes a short-range correlation when the orbital-disordered nanodomains appear. We consider that the orbital-disordered nanodomains interfere with the long-range ferromagnetic correlation.

1. Introduction

Perovskite-type manganites demonstrate many interesting electronic and structural properties [1]. Many manganites show various electronic ordered phases as a function of the hole-doping level x, such as, in many cases, a ferromagnetic metal phase via a double exchange interaction in underdoped manganites ($x \leqslant \sim 0.5$), and an antiferromagnetic (AF) charge/orbital

order, A-type AF and C-type AF insulator phases in overdoped manganites ($x \geqslant\sim 0.5$). In particular, the colossal magnetoresistance (CMR) effect, which is typically found in underdoped manganites, is one of the central issues in the study of strongly correlated electronic systems [2]. One of the well-known CMR mechanisms is the phase separation between two competing ordered phases around the phase boundaries [3]. However, there have not been many studies on overdoped manganites [4–6], apart from on the charge/orbital order manganites, although underdoped manganites have been studied extensively with the aim of understanding the CMR effect [1–3, 7–10]. However, Kajimoto *et al* [4] conducted pioneering research on an overdoped manganite, $Nd_{1-x}Sr_xMnO_3$ [4]. They revealed a systematic transformation of the crystal and magnetic structures in the $Nd_{1-x}Sr_xMnO_3$ ($0.49 \leqslant x \leqslant 0.75$) system, by neutron diffraction measurements. In almost all the underdoped region $x = 0.55$–0.75, the crystal structure above the Néel temperature of ∼200 K is tetragonal (space group (S.G.): $I4/mcm$). In the lower doping level, $x = 0.55$–0.63, the ground states are the A-type AF phase with $x^2 - y^2$-type and $z^2 - x^2$-type orbital order (OO). The crystal structures in the A-type AF phase depend on the OO structure. At $x = 0.55$, the crystal structure is orthorhombic (S.G.: $Ibmm$) with $x^2 - y^2$-type OO. At $x = 0.60$, on the other hand, Kajimoto *et al* (1999) supposed that the crystal structure is monoclinic (S.G.: $I112/m$) with $z^2 - x^2$-type OO [11]. In the higher doping level, $x = 0.63$–0.75, the ground state is the C-type AF phase with $3z^2 - r^2$-type OO, where the crystal structure is tetragonal (S.G.: $I4/mcm$). They also supposed that the phase boundary between the A-type and C-type AF phases is located around $x = 0.63$. Around the phase boundary, $x = 0.60$–0.70, a weak ferromagnetic phase appears below ∼50 K. Moreover, recent studies have revealed that overdoped $Nd_{1-x}Sr_xMnO_3$ crystals show unusual characteristics [5, 6, 12]. For $x = 0.55$–0.8, $3z^2 - r^2$-type OO evolves between 400 and 600 K, far above the Néel temperatures [5, 6]. Akahoshi *et al* have investigated the phase competition between the A-type AF phase and the C-type AF phase in $Nd_{1-x}Sr_xMnO_3$ crystals ($0.57 < x < 0.75$) [12]. They examined the texture for $x = 0.625$ by transmission electron microscopy (TEM) and then observed the tweed contrast between 5 and 470 K. The tweed structure is significant in the competition between different structures [13]. To clarify the relationship between the physical properties and the nanodomain leading to the tweed structure, detailed investigation of the nanodomain is necessary. In this study, we focused on the nanodomain and examined the crystal structures around the phase boundary by powder synchrotron x-ray diffraction (XRD) analysis and TEM. In addition, we investigated the magnetic domain structures in the weak ferromagnetic phase by Lorentz TEM to determine the relationship between the nanodomain and the magnetic property.

2. Experimental results and discussion

High-quality single crystals of $Nd_{1-x}Sr_xMnO_3$ ($x = 0.59$, 0.62, 0.625, 0.64 and 0.67) were grown by a floating-zone method, as described in detail elsewhere [5, 6]. Powder synchrotron XRD was performed using a high-resolution diffractometer with Debye–Scherrer geometry and an imaging-plate system as a detector installed at the BL-15XU beamline at SPring-8, Japan. The measurements were carried out at 120 and 300 K using a wavelength of 0.652 97 Å in the 2θ range between 8.0° and 44.5°. The samples were cooled by a cold nitrogen gas flow. All the data were analysed by the Rietveld method using the RIETAN-2000 program [14]. TEM experiments were carried out using a Lorentz microscope (HF-3000L) operating at 300 kV. The samples in the Lorentz microscope, which was equipped with a custom-made objective lens, were under almost zero magnetic field. For the observations, the specimens were cut into thin plates and then thinned by mechanical grinding followed by Ar^+ ion milling. We used the Fresnel method with the Lorentz TEM to image the magnetic domain structures [15]. The principle of imaging using the Fresnel method is described elsewhere [16].

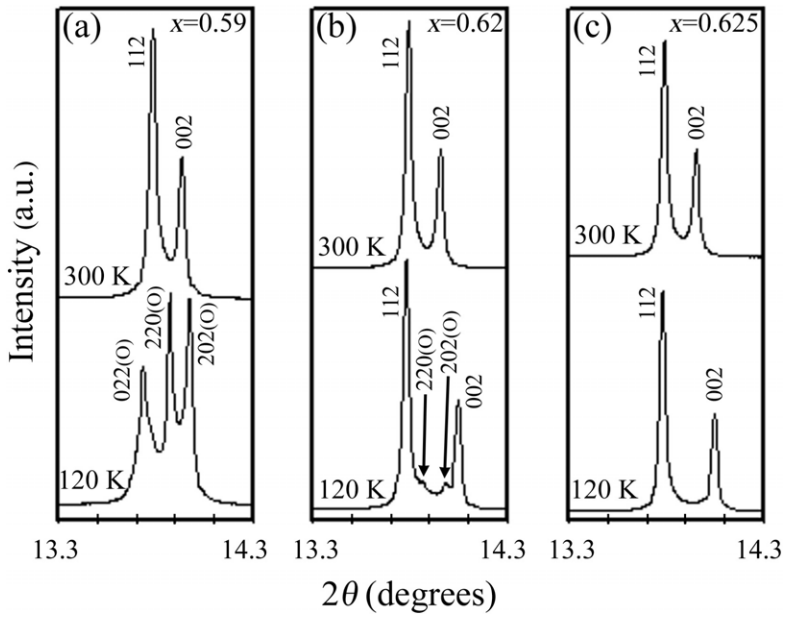

Figure 1. Parts of the powder synchrotron x-ray diffraction patterns at 120 and 300 K for $Nd_{1-x}Sr_xMnO_3$ with (a) $x = 0.59$, (b) $x = 0.62$ and (c) $x = 0.625$, respectively. The symbol (O) attached to the indexes denotes the peaks of the orthorhombic structure. The arrows in (b) indicate the peaks of the orthorhombic structure.

First, we investigated the average crystal structures by XRD analysis. Figures 1(a)–(c) show parts of the patterns at 120 and 300 K for $x = 0.59$, 0.62 and 0.625, respectively. The Rietveld refinements for all the patterns were successfully performed with the reliability factor R_{wp} being in the range from 3.01% to 5.21%. At 300 K, the crystal structure for all the compositions is the tetragonal $I4/mcm$ structure, which is consistent with the previous study [4]. The crystal structure for $x = 0.59$ changes to the orthorhombic $Fmmm$ structure at 120 K, which is induced by the $z^2 - x^2$-type OO running parallel to the {110} plane in the tetragonal setting [17], as shown in figure 1(a). Note that we could not fit both the monoclinic $I112/m$ and $P112_1/n$ structures [4, 11] and the orthorhombic $Ibmm$ structures [4]. The symbol (O) appended to the indexes in figures 1(a) and (b) denotes the peaks of the orthorhombic structure. For $x = 0.62$, figure 1(b) shows the phase separation of the tetragonal $I4/mcm$ structure with the C-type AF phase and the orthorhombic $Fmmm$ structure with the A-type AF phase at 120 K. From the Rietveld refinement, the mass fractions of the tetragonal $I4/mcm$ and orthorhombic $Fmmm$ phases are 82% and 18%, respectively. The crystal structure of $x = 0.625$ is tetragonal $I4/mcm$ at low temperature, as shown in figure 1(c). We confirmed macroscopically that this composition indicates the single C-type AF phase. Our XRD measurements provide convincing evidence that the phase boundary exists between $x = 0.62$ and 0.625.

Secondly, we examined the microscopic structure by TEM to determine the specific nature of the nanodomain. Figures 2(a)–(d) show the dark-field (DF) images formed using a 0 0 2 spot and the corresponding [010] zone-axis electron diffraction patterns (EDPs) obtained at room temperature for $x = 0.62$, 0.625, 0.64 and 0.67, respectively. We observed the tweed contrast at $x = 0.625$ and 0.64, as shown in figures 2(b) and (c), respectively. The tweed can certainly be observed everywhere on the ac plane. The $h\ 0\ l$ (h, l: odd) spots, which are forbidden

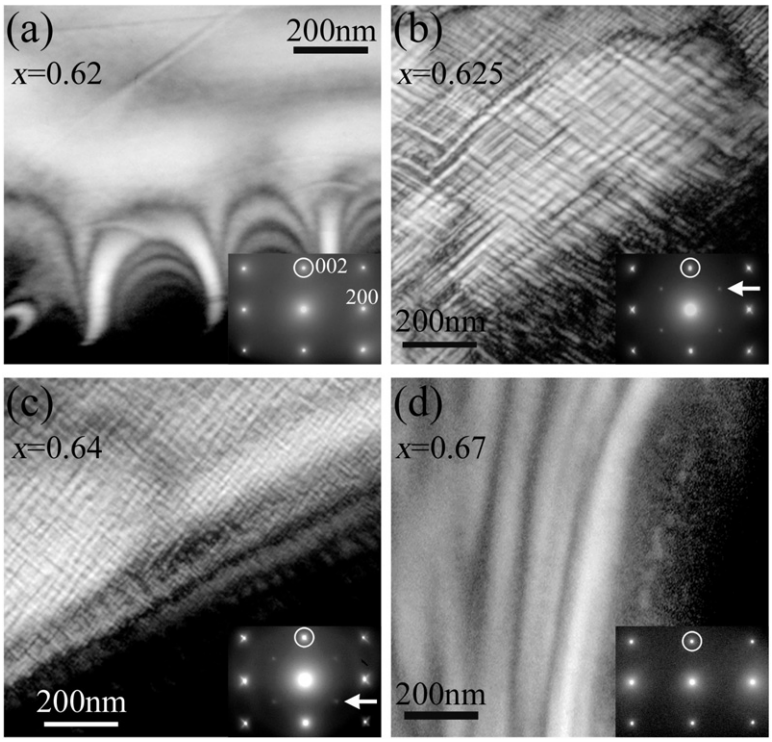

Figure 2. Dark-field images obtained using a 0 0 2 spot of $Nd_{1-x}Sr_xMnO_3$ for (a) $x = 0.62$, (b) $x = 0.625$, (c) $x = 0.64$ and (d) $x = 0.67$ at 300 K. The corresponding [010] zone-axis electron diffraction patterns, indexed on the basis of the tetragonal $I4/mcm$ structure, are shown in the corners of the respective figures. The 0 0 2 spots used for imaging are circled. The h 0 l (h, l = odd) spots, which appear as diffuse scatterings, are indicated by the arrows.

reflections for $I4/mcm$ symmetry, appear as diffuse scattering spots indicated by the arrows. The diffuse scattering spots indicate that nanodomains with a different structure exist within the tetragonal matrix phase. The tweed occurs as a consequence of the local lattice misfits between the tetragonal $I4/mcm$ ($3z^2 - r^2$-type OO) structure and the different structure of the nanodomains. On the other hand, there is no tweed contrast at $x = 0.62$ in the phase separation region and $x = 0.67$ far from the phase boundary, as shown in figures 2(a) and (d), respectively. The diffuse scattering spots also disappear. We could not observe the tweed contrast, even at 5 K, for these values of x. The results indicate that the nanodomain exists only in the vicinity of the phase boundary in the C-type AF phase. The appearance of the nanodomain is a characteristic phenomenon at the phase boundary between the A-type and C-type AF phases in the $Nd_{1-x}Sr_xMnO_3$ system. In the EDP for $x = 0.625$, which is rotated about $\langle 101 \rangle$ from the [010] zone-axis by a few degrees, the diffuse scattering spots disappear (not shown in the figure). This indicates that the diffuse h 0 l ($h = l$ or $h = -l$: odd) spots are caused by double diffraction. On the basis of the extinction rule of diffraction, the nanodomain structure is assigned to rhombohedral $R\bar{3}c$, which is an orbital-disorder structure for manganites.

Figure 3(a) shows DF image for $x = 0.625$, formed using a fundamental 0 0 2 spot at room temperature. The image shows tweed contrast similar to that observed in figures 2(b) and (c). On the other hand, figure 3(b), which is obtained using a diffuse 1 0 3 spot, clearly displays nanodomains with a size of 10–20 nm. The DF images are direct evidence of the presence of

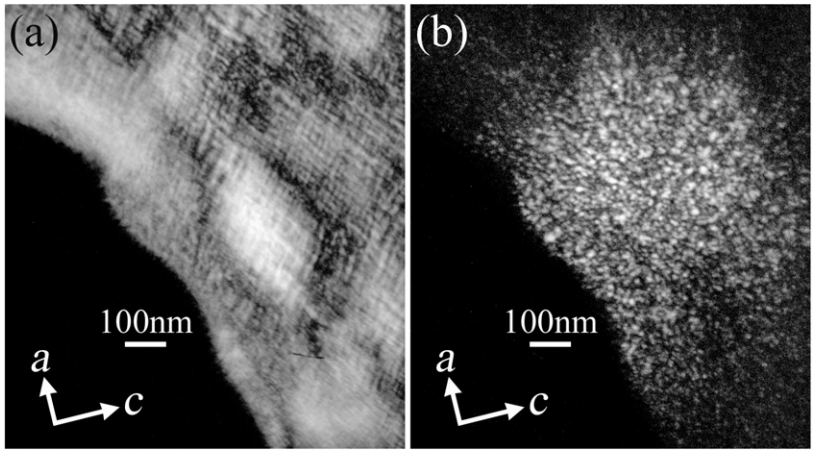

Figure 3. Dark-field images of (a) the tweed and (b) the nanodomains in $Nd_{1-x}Sr_xMnO_3$ ($x = 0.625$) at 300 K, obtained using a 0 0 2 spot and a diffuse 1 0 3 spot, respectively.

rhombohedral (orbital-disordered) nanodomains in the tetragonal ($3z^2 - r^2$-type OO) matrix phase.

We investigated the magnetic domain structure in the weak ferromagnetic phase to determine the relationship between the magnetic property and the nanodomain. Figures 4(a)–(d) show the Lorentz–Fresnel images for $x = 0.62$, 0.625, 0.64 and 0.67, respectively, at 5 K. Black and white lines in the images indicate magnetic domain walls. Each magnetic domain is surrounded by a pair of black and white lines. At $x = 0.62$ and 0.67, the magnetic domains are clearly observed, as shown in figures 4(a) and (d), respectively. At $x = 0.67$, we observed many domain walls located at the twin boundaries. It is well known that the magnetic domain wall of manganites is pinned strongly at the twin boundaries [18, 19]. On the other hand, at $x = 0.625$ and 0.64, no magnetic domains could be observed, as shown in figures 4(b) and (c). These figures indicate that the compositions with the nanodomain do not have a long-range magnetic order. These results are direct evidence that the magnetic property changes from long-range to short-range correlations when the nanodomains appear. Namely, the nanodomains affect the macroscopic magnetic property.

Akahoshi *et al* discovered a concomitant large magnetoresistance in accordance with the intensity of the magnetic susceptibility in the weak ferromagnetic phase [12]. In particular, the magnetic susceptibility and magnetoresistance are most enhanced at $x = 0.625$. The enhancement could be due to the emergence of the nanodomain. There are two possible causes of the magnetoresistance due to the presence of the nanodomains. One is the melting of both the nanodomain and the C-type AF insulator phase, the other is the expansion of the orbital-disordered nanodomain into the C-type AF insulator phase. Unfortunately, we were unable to determine the cause using experimental techniques.

Our observed phenomena are reminiscent of relaxor ferroelectrics [20, 21], whose origin and properties are the subject of controversy. Relaxor ferroelectrics emerge as a distinct phase in the balance between non-ferroelectric phases and conventional ferroelectric phases [20]. It is widely thought that local nanometre-scale polarized regions, termed polar nanoregions (PNRs), play a critical role in the physical properties of relaxor ferroelectrics [22]. The PNRs appear at higher temperatures, the so-called Burns temperature [22], which is much higher than ferroelectric transition temperatures. The PNRs do not indicate macroscopic spontaneous polarization. However, compositions in the presence of the PNRs exhibit an anomalously large

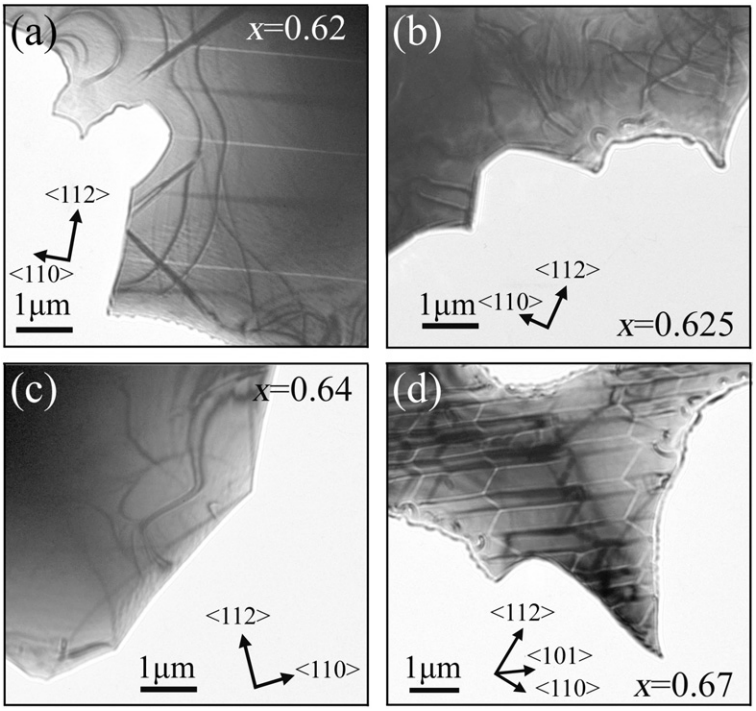

Figure 4. Fresnel images of $Nd_{1-x}Sr_xMnO_3$ for (a) $x = 0.62$, (b) $x = 0.625$, (c) $x = 0.64$ and (d) $x = 0.67$ at 5 K. The black and white lines indicate magnetic domain walls for (a) $x = 0.62$ and (d) $x = 0.67$. The magnetic domain walls for (d) $x = 0.67$ are pinned at the twin boundaries, which are parallel to $\langle 101 \rangle$. No magnetic domains for (b) $x = 0.625$ and (c) $x = 0.64$ are observed.

dielectric susceptibility below the Burns temperature. It is interesting that PNRs persist down to lower temperatures, at which they coexist with a long-range ferroelectric phase with different symmetry [23], similar to the behaviour observed in this study. The nanodomains appear only in the vicinity of the phase boundary and persist down to the low temperature of 5 K. They also coexist with the $3z^2 - r^2$-type OO matrix phase of different crystal structure. In the presence of the nanodomains, the ferromagnetic correlation becomes a short-range correlation. The nanodomains play an essential role in the physical properties of overdoped $Nd_{1-x}Sr_xMnO_3$ crystals.

In summary, we have revealed the specific nature and role of the nanodomains by transmission electron microscopy and powder synchrotron x-ray diffraction. The nanodomains only exist in the vicinity of the phase boundary. We have also revealed that the nanodomains are indirectly connected with the ferromagnetic correlation through the $3z^2 - r^2$-type OO matrix phase. The ferromagnetic correlation becomes short range when the nanodomains appear. The compositions in the presence of the nanodomains have a distinct phase from the other phases of hole-doped manganites. This novel phase is characterized by a nanoscale inhomogeneity but is not a phase separation which has been the much-discussed subject of the colossal magnetoresistance effect.

Acknowledgments

We thank C Tsuruta, W Z Zhang, Y Katsuya and H Tanaka for their help with the TEM and XRD experiments and X Z Yu, T Yokosawa, Y Matsushita and A Yamamoto for the fruitful

discussions. Part of this work was supported by the Nanotechnology Support Project of the Ministry of Education, Culture, Sports, Science and Technology (MEXT), Japan. TA was supported by the Japan Society for the Promotion of Science (JSPS) for Young Scientists. HK was supported by a Grant-in-Aid for Scientific Research (C) from JSPS, and by a Grant-in-Aid for Scientific Research on Priority Areas (No. 451) from MEXT, Japan.

References

[1] Imada M, Fujimori A and Tokura Y 1998 *Rev. Mod. Phys.* **70** 1039
[2] Jin S, Tiefel T H, McCormack M, Fastnacht R A, Ramesh R and Chen L H 1994 *Science* **264** 413
[3] Uehara M, Mori S, Chen C H and Cheong S-W 1999 *Nature* **399** 560
[4] Kajimoto R, Yoshizawa H, Kawano H, Kuwahara H, Tokura Y, Ohoyama K and Ohashi M 1999 *Phys. Rev.* B **60** 9506
[5] Tobe K, Kimura T and Tokura Y 2003 *Phys. Rev.* B **67** 140402
[6] Kuwahara H, Kawasaki R, Hirobe Y, Kodama S and Kakishima A 2003 *Physica* B **329–333** 850 Part 2
[7] Hwang H Y, Cheong S-W, Radaelli P G, Marezio M and Batlogg B 1995 *Phys. Rev. Lett.* **75** 914
[8] Radaelli P G, Iannone G, Marezio M, Hwang H Y, Cheong S-W, Jorgensen J D and Argyriou D N 1997 *Phys. Rev.* B **56** 8265
[9] Adams C P, Lynn J W, Mukovskii Y M, Arsenov A A and Shulyatev D A 2000 *Phys. Rev. Lett.* **85** 3954
[10] Salamon M B, Lin P and Chun S H 2002 *Phys. Rev. Lett.* **88** 197203
[11] Llobet A, Garcia-Munoz J L, Frontera C and Ritter C 1999 *Phys. Rev.* B **60** R9889
[12] Akahoshi D, Hatakeyama R, Nagao M, Asaka T, Matsui Y and Kuwahara H 2007 Anomalous ferromagnetic behavior and large magnetoresistance induced by orbital fluctuation in heavily-doped $Nd_{1-x}Sr_xMnO_3$ ($0.57 \leqslant x \leqslant 0.75$) *Phys. Rev.* B submitted
[13] Parlinski K, Heine V and Salje E 1993 *J. Phys.: Condens. Matter* **5** 497
[14] Izumi F and Ikeda T 2000 *Mater. Sci. Forum* **321–324** 198
[15] Yu X Z, Asaka T, Tomioka Y, Tsuruta C, Nagai T, Kimoto K, Kaneko Y, Tokura Y and Matsui Y 2005 *J. Electron. Microsc.* **54** 61
[16] Grundy P J and Tebble R S 1968 *Adv. Phys.* **17** 153
[17] Raveau B, Hervieu M and Maignan A 2000 *Phys. Rev.* B **62** 6820
[18] Asaka T, Anan Y, Nagai T, Tsutsumi S, Kuwahara H, Kimoto K, Tokura Y and Matsui Y 2002 *Phys. Rev. Lett.* **89** 207203
[19] Mori S, Asaka T, Horibe Y, Matsui Y and Takenaka K 2005 *J. Electron. Microsc.* **54** (Suppl. 1) I65–8
[20] Cross L E 1987 *Ferroelectrics* **76** 241
[21] Noheda B, Cox D E, Shirane G, Park S-E, Cross L E and Zhong Z 2001 *Phys. Rev. Lett.* **86** 3891
[22] Burns G and Dacol F H 1983 *Solid State Commun.* **48** 853
[23] Xu G Y, Zhong Z, Bing Y, Ye Z-G and Shirane G 2006 *Nat. Mater.* **5** 134